Supplementary Information

Revealing the Intrinsic Peroxidase-Like Catalytic Mechanism of O–doped CoS_2 Nanoparticles

Shufeng Liang[‡a,b], Tingyu Chen[‡c], Yun Zhao[c], Yali Ren[a], Miaomiao Li[a], Dongtao Lu[a], Junhao Wang[d], Yan Dai*[a], Yujing Guo*[a]

[a] Institute of Environmental Sciences, Shanxi University, Taiyuan 030006, China; [b] Department of Clinical Laboratory, Shanxi Province Cancer Hospital/Shanxi Hospital Affiliated to Cancer Hospital, Chinese Academy of Medical Sciences/Cancer Hospital Affiliated to Shanxi Medical University, Taiyuan 030013, China; [c] School of Environment and Energy, Guangdong Provincial Key Laboratory of Atmospheric Environment and Pollution Control, South China University of Technology, Guangzhou 510000, China; [d] Institute of crystalline materials, Shanxi University, Taiyuan 030006, China.

.

‡These authors contributed equally to this work.

*Corresponding author: E-mail: ydai@sxu.edu.cn (Yan Dai), guoyj@sxu.edu.cn (Yujing Guo)

S1. Materials and methods

Chemicals and materials

CoCl$_2$·6H$_2$O and tartrazine (> 95%) were purchased from Shanghai Aladdin Biochemical Technology Co., Ltd. (Shanghai, China). Na$_2$S$_2$O$_3$·5H$_2$O (> 99%) was obtained from Alfa Aesar (China). MeOH (99.9%), Hydrogen peroxide (H$_2$O$_2$, 30%), and Methylene blue (MB) were purchased from Beijing Innochem Science & Technology Co., Ltd. (Beijing, China). 5,5-Dimethyl-1-pyrroline N-oxide (DMPO, ≥ 99%) was purchased from Dojindo China Co., Ltd. (Shanghai, China). 3,3,5,5-Tetramethylbenzidine (TMB) and terephthalic acid (TA, 98%) were obtained from Sigma-Aldrich (St. Louis, MO, U.S.A.). Rhodamine B (RhB) was obtained from Beijing Hua Gong Chang (Beijing, China). All chemicals and reagents were analytical grade and used as received without further purification. Ultrapure water (18.2 MΩ) was used throughout the experiment.

Characterizations

The powder X-ray diffraction (PXRD) measurements were performed on a Rigaku Ultima IV diffractometer using Cu Kα radiation and graphite monochromator (λ=1.54056 Å) at 40 kV voltage and 40 mA current at the scan speed of 10 ^{o}/min with a step size of 0.02^{o}. FEI Tecnai G2 F20S-TWIN transmission electron microscopy (TEM, USA) operating at 200 kV was used to observe the morphology of the O-doped CoS$_2$ NPs. The High-resolution TEM (HRTEM) was applied for the identification of the lattice spacing of the O-doped CoS$_2$ NPs. The X-ray photoelectron spectroscopy (XPS) was performed on an ESCALAB 250Xi instrument (Thermo Fischer, USA), and the C$_{1s}$ line at 284.8 eV was used as the binding energy reference. Thermo Scientific Avantage software version 5.9922 was used to fit peaks. A mixed Gaussian (30%)–Lorentzian (70%) product function was used to fit the peaks after background subtraction. A smart Shirley function was used to subtract the background when fitting Co 2p, S 2p, O 1s, and C 1s peaks. To assess the sulfur or oxygen vacancy of nanozymes, electron paramagnetic resonance measurements (EPR, Bruker-A300) were carried out using a Bruker EMXPLUS10/12 EPR spectrometer.

Materials preparation

O-doped CoS$_2$ NPs were successfully synthesized by the hydrothermal method. Typically, 1.0 mmol of CoCl$_2$·6H$_2$O and 2.0 mmol of Na$_2$S$_2$O$_3$·5H$_2$O were fully dissolved in 30 mL ultrapure water. The mixture was placed in a polytetrafluoroethylene (PTFE) vessel (inner volume 50 cm^3). The vessel was sealed, placed in a stainless-steel autoclave, and kept at 180 °C (oven temperature) for 12 h under autogenous pressure. After the reaction, the autoclave was cooled naturally to room temperature. Further, the black precipitate was collected by centrifugation of the mixture solution at 8,000 r/min for 10 minutes and washed three times with ultrapure water, ethanol, and trichloromethane, separately. After drying the washed sample in a vacuum drying oven at 60 $^\circ$C for four hours, the final products were stored in a dryer for further use.

The catalytic kinetics of O-doped CoS$_2$ NPs

Kinetic measurements were carried out in a 1 mL solution containing nanozymes (2 mg mL^{-1}, 20 μL) and varying concentrations of TMB and H$_2$O$_2$ in NaAc/HAc buffer (pH 3.6) solution at room temperature. Thirty seconds later, color reactions were recorded in a time-scan mode at 10 s intervals for one minute by monitoring the absorbance at 652 nm. The initial rate of change of absorbance was determined by plotting the absorbance against the reaction time and measuring the slope of the resultant straight lines.

Kinetic constants Michaelis constant (K_m) and maximal reaction rate (v_{max}) were calculated by plotting initial reaction velocity (v) against substrate concentration and fitting plots with the Michaelis-Menten equation using GraphPad Prism 7.0 software. The Michaelis-Menten equation is as follows:

$$v = v_{max} \times [S]/(K_m + [S]) \qquad \text{(Eq. 1)}$$

Here, v is initial reaction velocity; v_{max} is maximal reaction rate; [S] is substrate concentration; and K_m is Michaelis constant.

The stability tests of O-doped CoS$_2$ NPs

Firstly, 32 μmol of O-doped CoS$_2$ NPs were incubated in 2 mL of reaction buffer (pH 3.6) for 30 min. Then, the precipitate was achieved by centrifugation at 8000 rpm for 5 min and the leaching solution was collected. The POD-like activities of different catalysts were compared under the same conditions. O-doped CoS$_2$ NPs (16 mM, 50 μL), or the precipitate solution (dispersed in 2 mL of ultrapure water, 50 μL), or the leaching solution (50 μL), or Co (NO$_3$)$_2$ (16

mM, 50 μL) were added into NaAc/HAc buffer solution (pH 3.6) containing 1 mM TMB and 100 mM H_2O_2 at room temperature, respectively. The final volume of the reaction solution was 1 mL.
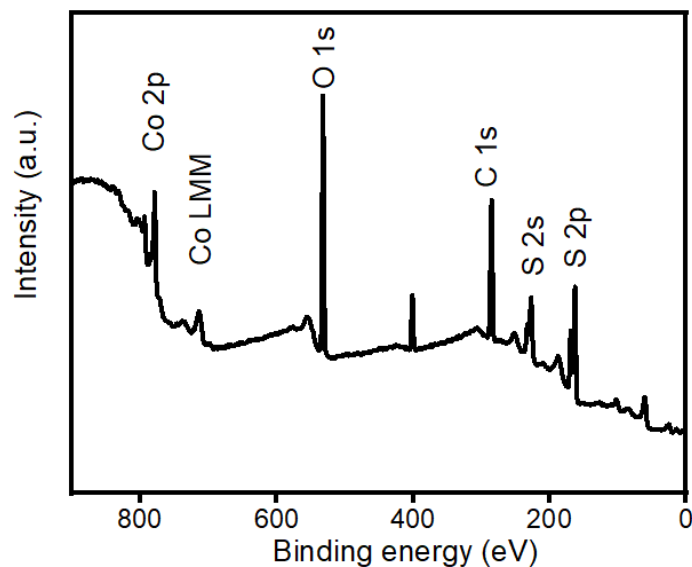
S2. Figures

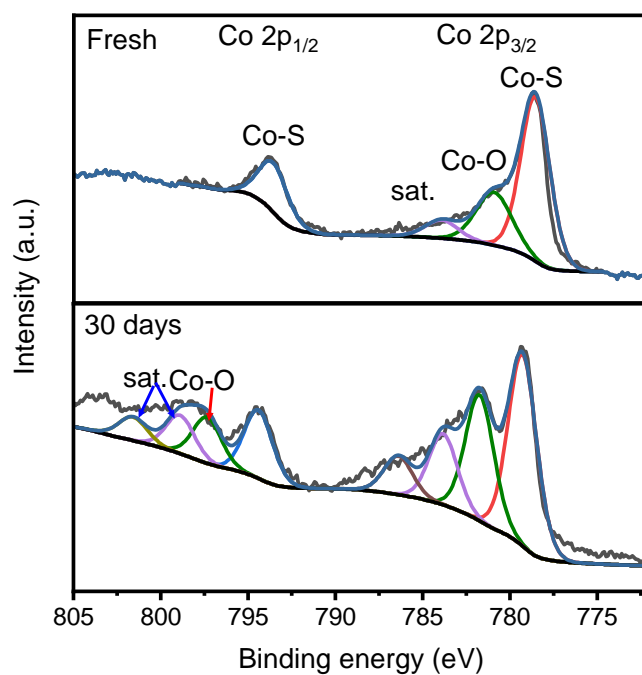Figure S1. XPS survey spectra for O-doped CoS$_2$ NPs.

Figure S2. Comparation of XPS spectra in the Co 2p regions of fresh O-doped CoS$_2$ NPs and ox-CoS$_2$ NPs (after 30 days of storage).

For fresh O-doped CoS$_2$ NPs, the peak at 780.9 eV (2p$_{3/2}$) is attributed to the Co-O bond and the missing of Co 2p$_{1/2}$ peak for Co-O bond possibly due to the low content of the Co-O species on the surface. The Co-O/Co-S surface ratio of fresh O-doped CoS$_2$ NPs is 25:75. While for the sample after 30 days of storage, it changed to 40:60. In this case, the peak of Co 2p$_{1/2}$ at 797.35 eV

belong to Co-O bond appeared.
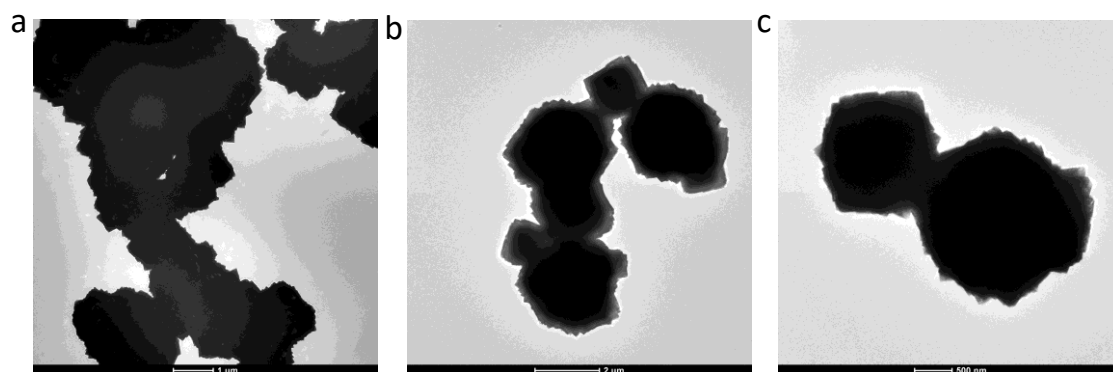
Figure S3. The TEM images of O-doped CoS_2 NPs.
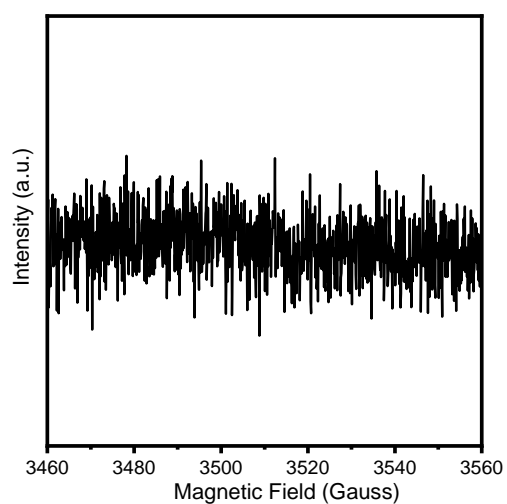
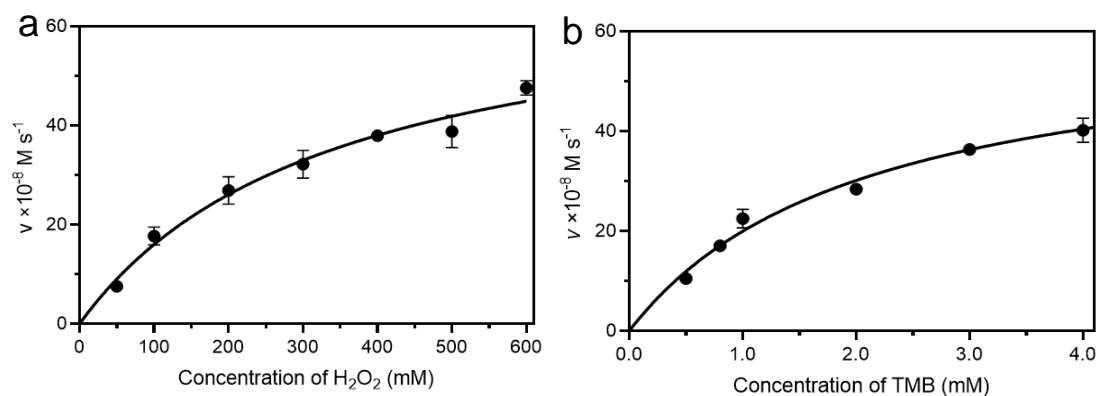Figure S4. EPR spectrum of O-doped CoS_2 NPs at room temperature.

Figure S5. The kinetic assay for the POD-like activity of O-doped CoS_2 NPs by varying the concentration of TMB or H_2O_2 and fixing the other. (a) The concentration of H_2O_2 (10 M, 50 µL) was fixed at 500 mM and the concentration of TMB was varied. (b) The concentration of TMB (40 mM, 75 µL) was fixed at 3 mM and the concentration of H_2O_2 was varied (n = 3, bars represent means ± standard deviations). All of the experiments were carried out in NaAc/HAc buffer (0.2 M:0.2 M, pH 3.6) at room temperature.

Table S1 Catalytic kinetic parameters of O-doped CoS_2 NPs.

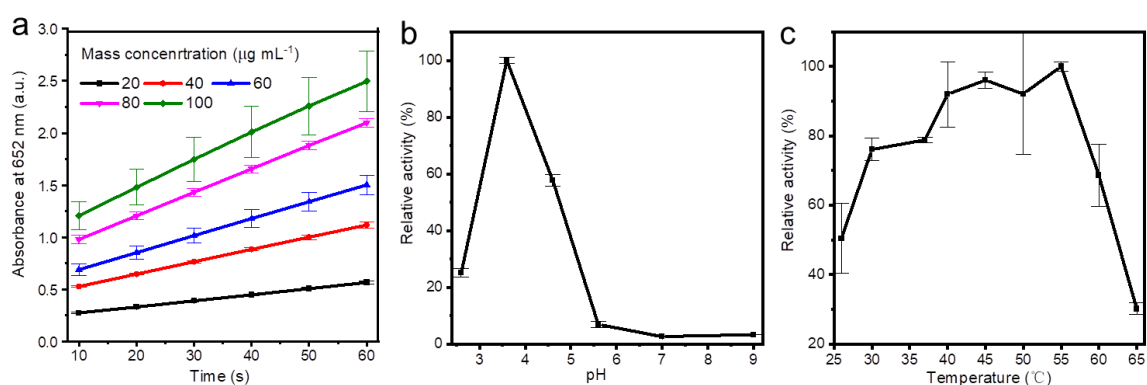| Catalyst	Substrate	K_m (mM)	v_{max} (10^{-8} M s^{-1})
O-doped CoS_2 NPs	TMB	2.08	61.5
	H_2O_2	339	70.3

Figure S6. The effects of mass concentration (a), pH (b), and temperature (c) on the catalytic activity of O-doped CoS_2 NPs.
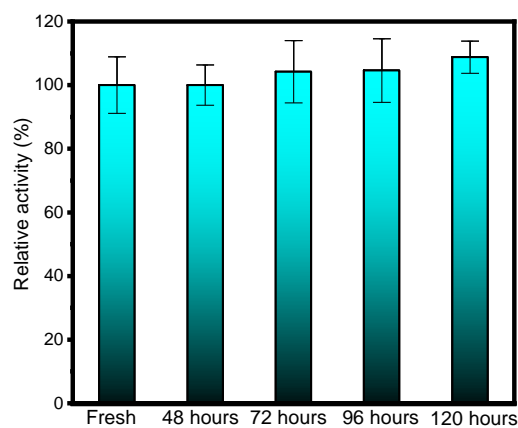
Figure S7. The POD-like activities of O-doped CoS_2 NPs after incubating in HAc/NaAc buffer solution for different time scales.
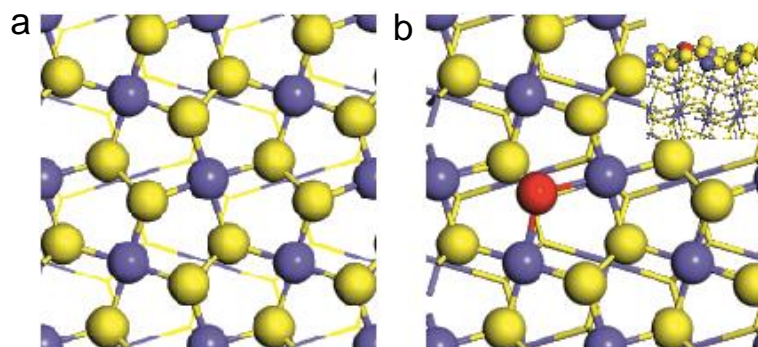

Figure S8. Geometrical structures of (a) $CoS_2(001)$, (b) O-doped $CoS_2(001)$ (one surface S atom replaced by O atom) surfaces.
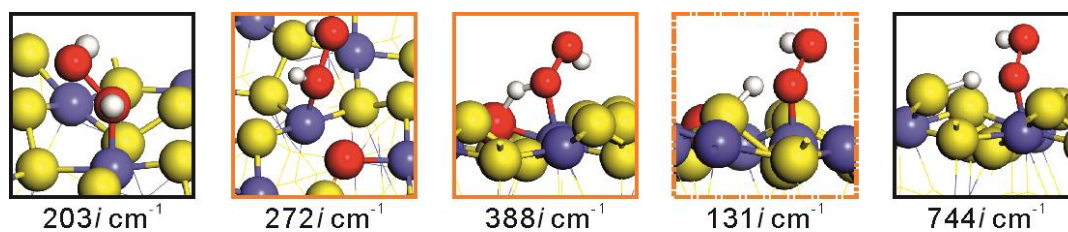

$203i\,cm^{-1}$ $272i\,cm^{-1}$ $388i\,cm^{-1}$ $131i\,cm^{-1}$ $744i\,cm^{-1}$

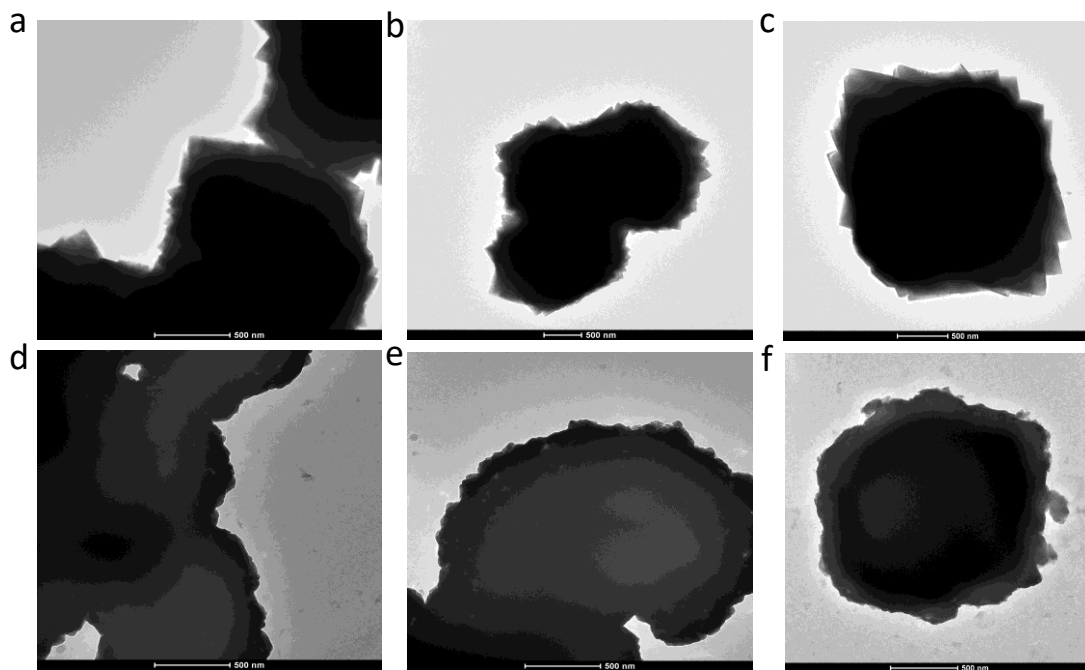Figure S9. Calculated negative frequencies of transition states in the pathway shown in Figure 4.

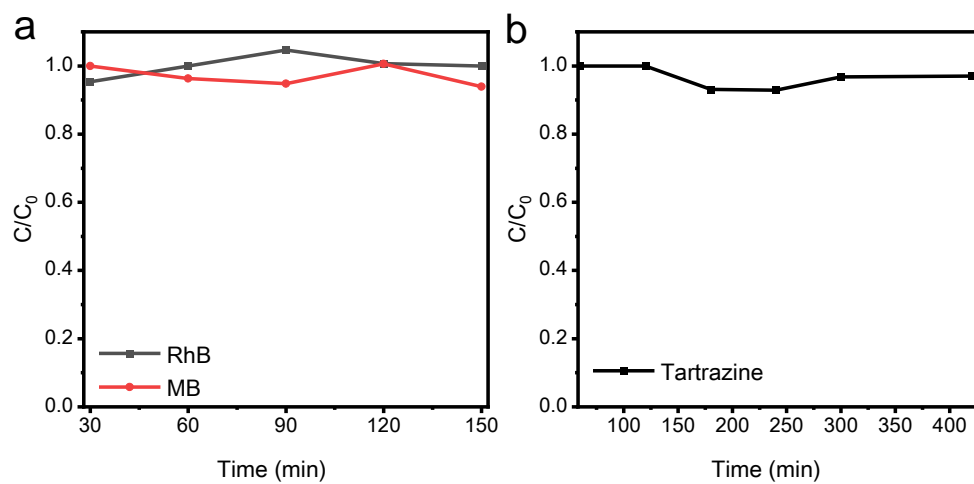Figure S10. The TEM images of O-doped CoS_2 NPs (a-c) and the one after 21 days of storage (d-f).

Figure S11. The adsorption of dyes by O-CoS_2 NPs.

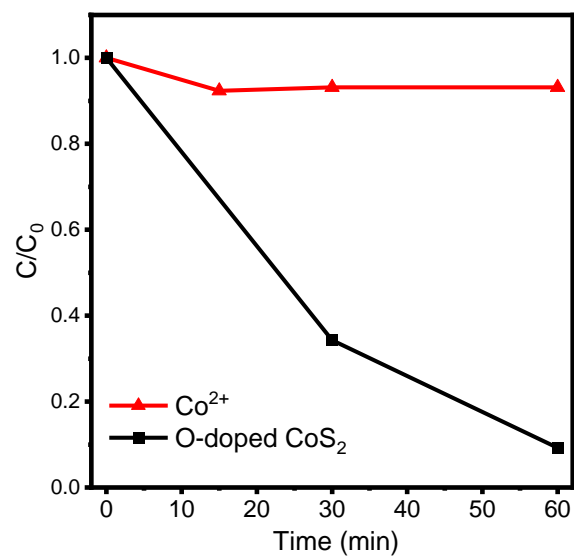Figure S12. Comparison of the catalytic degradation rate of MB by Co^{2+}/H_2O_2 system or O-doped CoS_2 NPs/H_2O_2 system. Reaction conditions: Co^{2+} or O-doped CoS_2 NPs 8 mM, H_2O_2=100 mM, [MB]=10 mg L^{-1}, pH=4.0, temperature=20 °C.